Polymer 52 (2011) 1954–1962

Contents lists available at ScienceDirect

Polymer

journal homepage: www.elsevier.com/locate/polymer

Ionic liquid assisted electrospinning of quantum dots/elastomer composite nanofibers

Jiahua Zhu [a], Suying Wei [b], Rahul Patil [a], Dan Rutman [a], Ashwini S. Kucknoor [c], Andrew Wang [d], Zhanhu Guo [a,*]

[a] Integrated Composites Laboratory (ICL), Dan F. Smith Department of Chemical Engineering, Lamar University, Beaumont, TX 77710, USA
[b] Department of Chemistry and Biochemistry, Lamar University, Beaumont, TX 77710, USA
[c] Department of Biology, Lamar University, Beaumont, TX 77710, USA
[d] Ocean NanoTech, LLC, 2143 Worth Ln., Springdale, AR 72764, USA

ARTICLE INFO

Article history:
Received 18 January 2011
Received in revised form
21 February 2011
Accepted 28 February 2011
Available online 8 March 2011

Keywords:
Polymer nanocomposites
Elastomer fibers
Fluorescence

ABSTRACT

Quantum dots (QDs)/elastomer (VM) composite nanofibers have been fabricated via electrospinning method with the assistance of small amount (1 wt%) of ionic liquid. Without ionic liquid, polymer solution underwent an electrospraying process within the electric field and only individual droplets rather than continuous fibers were observed. Both fixed electrode and rotating disk electrode were used to collect the products. The latter one turned out to be much more advanced in collecting separated, aligned and narrow-size distributed composite nanofibers. With fixed electrode, even though nanofibers were obtained initially, the as-spun fibers were easily to merge together due to the flexible non-crystalline nature of the VM chains and finally formed a condensed thin film. Strong fluorescent emission was observed in the composite nanofibers with a QD loading of 3 and 5 wt%, respectively. The optical property of QDs was not degraded after dispersing in the polymer solution as evidenced by the UV–Vis absorption at 562 nm and 592 nm, and strong photoluminescent emission at 612 nm. In addition, differential scanning calorimetry (DSC) analysis revealed a strong interaction between ionic liquid and the polymer chains, which well explains the function of the ionic liquid on producing fiber structure of VM. An enhanced thermal stability of the elastomer in the composite nanofibers is observed as compared to that of the pure elastomer fibers.

1. Introduction

Electrospinning technology has received growing interest recently owing to its comparatively low manufacturing cost and high yield for fabricating polymer fibers with diameters ranging from micrometers down to a few nanometers [1–4]. In a typical process, a polymer solution is forced through a syringe pump, forming a pendent drop at the tip of capillary. When the applied electric field strength (between the needle tip and the grounded collecting electrode) overcomes the surface tension force and viscoelastic force of the droplet, a polymer solution jet is initiated and accelerated toward the collecting electrode. As the jet travels through the air, the solvent evaporates and a non-woven polymeric fabric is formed on the target [5]. The resulting electrospun non-woven fibers possess a large specific surface area, high porosity and small pore size, which have equipped them vast potential applications such as gas separation [6], protein purification [7], scaffoldings for tissue engineering [8,9] and nano-electronics [10].

Viscoelastic elastomers, generally having high yield strain and low Young's modulus, have been used in electrical actuators [11], adhesives [12] and soft tissue replacements [13] because of their high toughness and long-term durability. Ultrafine polymer fibrous structures become even more attractive for their potential applications in filtration [7,14], wound dressing [15], drug delivery [16,17] and tissue scaffolds [18,19] after Reneker and co-workers developed new interest of electrospinning in 1990s due to their high specific surface area and the introduced unique physico-chemical properties. After that, large amount of different polymer fibers have been produced using the electrospinning method in the last two decades, including polyimide [1], polyacrylonitrile (PAN) [2], polyvinyl alcohol (PVA) [20], polystyrene (PS) [21] and etc. More detailed information regarding the polymer fiber species and electrospinning design would refer to the recent literature reviews [22,23]. However, it is really a challenge to electrospin elastomers into stable micron- and nano-fibers because of their low glass transition temperature and viscous surface, which make the

* Corresponding author. Tel.: +1 409 880 7654.
E-mail address: zhanhu.guo@lamar.edu (Z. Guo).

0032-3861/$ – see front matter © 2011 Elsevier Ltd. All rights reserved.
doi:10.1016/j.polymer.2011.02.051

as-spun fibers merge quickly into large fibers or even a continuous thin film [24]. To solve this problem, researchers tried to blend the elastomer with a polymer, such as polyacrylonitrile [25], which can be easily electrospun. However, this could not be a general solution through simple mixing because most polymers are incompatible or immiscible. Even though some strategies have been attempted to compatiblize the immiscible polymer blends through interlocking both polymers into a "interpenetrating network" [26], it is still hard to control the solution property (like cross linking density and viscosity) for electrospinning.

The semiconductive nanocrystals, known as quantum dots (QDs), have become a rapidly growing research area due to their unique size-dependent optical and electronic properties [27]. Applications of QDs in solar cells [28], light emitting diodes (LEDs) [29] and bio-probes in sensing and imaging [30–33] have intrigued great interest worldwide during the last decade. Recently, QDs have shown the ability to generate multiple electron-hole pairs per photon, which would greatly improve the efficiency of the photovoltaic devices [34,35]. In biology science, labeling molecules using organic fluorescent tags is a common and very useful practice in cellular imaging, drug delivery and nano-sensing [36,37]. QDs are preferred in certain fluorescent tagging applications by combining advantages of high photobleaching threshold, good chemical stability and readily tunable spectral properties [30]. Meanwhile, numerous cell studies have also been successfully carried out on the electrospun polymer fibers [38–40].

Polymer nanocomposites (PNCs) are of great interest recently owing to their novel properties derived from the successful combination of the characteristics of parent constituents into a single material. The unparallel advantages of PNCs, such as cost-effective processability, light weight, and tunable mechanical, magnetic, and electric properties [41–43] make them promising materials in wide applications. QDs have been demonstrated to be effective nanofillers in polymers to design composite sub-wavelength optical waveguides [44] and efficient photoconductive devices at infrared length [45]. The elastic nature of the elastomer fibers/nanofibers could be very promising in muscle reconstruction and replacement [46,47]. Combining with the fluorescent tagging of QDs embedded in the elastomer fibers, the cell integration and dynamic mobility can be traced more easily and precisely. However, rare work has been reported until now on the fabrication of fluorescent composite nanofibers, which may improve the efficiency and sensitivity in cell separation and diagnostic applications.

Ionic liquid, a newly developed solvent, with particular advantages such as excellent dissolution ability, high thermal stability and easy recycling, has been identified to have great potential applications such as serving as a green solvent for textile industry [48,49] and for fabricating monodispersed nanoparticles [50]. Among different ways to improve the electrospinnability of different materials including mixed solvent (tetrahydrofuran (THF)/dimethylformamide (DMF)) [51], blended polymer (elastomer/polyacrylonitrile) [25], and inorganic salt (NaCl, $Fe(NO_3)_3$) [20], ionic liquid as a strong electrolyte and its capability to dissolve polar and non-polar compounds could have great potential to facilitate electrospinning process by increasing the ionic strength of the polymer solution, as well as expanding the selection of materials. To the best of our knowledge, only a few works have been done on the electrospinning using ionic liquid to enhance the electrospinnability of polymers. Recently, Li et al. [52] reported electrospun polystyrene nanofibers with superhydrophobicity and conductivity containing ionic liquid. Biopolymer fibers (cellulose and cellulose-heparin composite fibers) are also produced using room temperature ionic liquid as solvent [53]. In this work, small amount of ionic liquid, 1-Decyl-3-methylimidazolium-tetrafluoroborate, has been introduced to the polymer solution to facilitate the electrospinning process via increasing ionic intensity. Without ionic liquid, it is almost impossible to obtain fiber structure from the regular elastomer/toluene solutions. Fluorescent elastomer/QDs composite nanofibers are successfully produced. As compared with the network structured composite nanofibers spun from a fixed ground collector, well-aligned electrospun fibers are fabricated by using a rotating disk electrode. Strong emission observed in the fluorescence microscope demonstrates that the QDs are well distributed in the electrospun composite nanofibers. Enhanced thermal stability is also obtained in the composite nanofibers as compared to that of the pure polymer fibers.

2. Experimental

2.1. Materials

Vistamaxx 6202 propylene based elastomer (VM) with an ethylene content of 15 wt% is provided by ExxonMobil Chemical Company. Core/shell cadmium selenide (CdSe)/zinc sulfide (ZnS) quantum dots (QDs, ~5 nm) coated with octadecylamine are supplied by Ocean NanoTech LLC. Fig. 1a shows the high resolution TEM image of the QDs with clear lattice fringes, indicating a highly crystalline structure of the QDs. 1-Decyl-3-methylimidazolium-tetrafluoroborate ionic liquid (IL, $C_{14}H_{27}BF_4N_2$, M_w: 310.18 g/mol,) is purchased from Sigma Aldrich. Fig. 1b shows the molecular structure of ionic liquid. All the chemicals are used as-received without any further treatment.

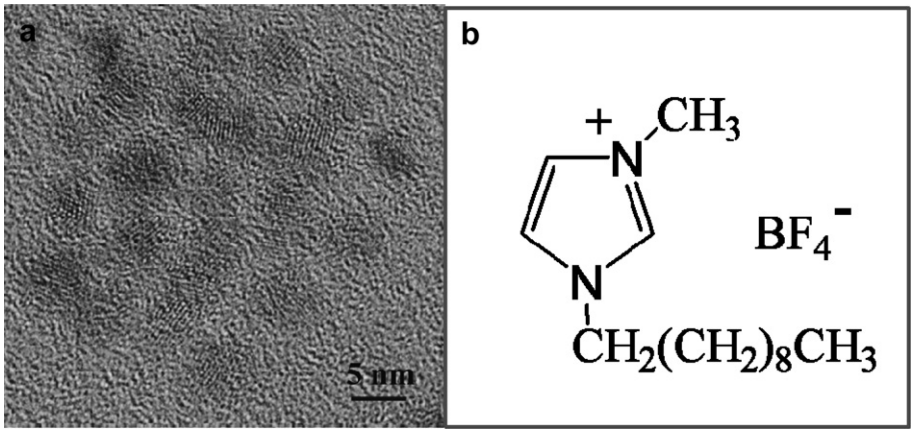

Fig. 1. (a) HRTEM microstructure of the CdSe–ZnS core-shell quantum dots and (b) the molecular structure of ionic liquid used in this work.

2.2. Preparation of VM and QDs/VM nanocomposite solutions

The VM/toluene solutions with VM loadings of 8, 10 and 12 wt% are prepared by magnetic stirring at 70 °C for 6 h to completely dissolve the polymer. Based on the observations during the fiber fabrication, solution with an elastomer loading of 12 wt% is the optimal concentration for electrospinning. Therefore, QDs/VM nanocomposite solutions are prepared from 12 wt% elastomer solution. To be specific, 4.80 g VM is dissolved in 36 mL toluene by magnetically stirring at 70 °C for 6 h. QDs are dispersed in 5 mL toluene with different weight (0.5, 1, 3 and 5 wt%, with regard to the weight of VM) under ultrasonication for 15 min. The QD solutions are added dropwise to the polymer solution while keep stirring. The above solution is stirred for additional 2 h at room temperature. To increase the ionic strength of the polymer solutions and hence enhance the electrostatic forces of the fluid during electrospinning, 0.048 g ionic liquid (1 wt% of the polymer) is added to each solution. The ionic strength of the solution is estimated from the following equation:

$$I = \frac{1}{2}\sum_{i=1}^{n} C_i Z_i^2 \quad (1)$$

where I is the ionic strength, a function of the concentration of all ions present in the solution. C_i is the molar concentration of ion i (mol dm^{-3}), Z_i is the charge number of the ion i. The estimated ionic strength is 3.32 mmol/L for each solution.

2.3. Fabrication of VM and QD/VM composite nanofibers

Pure VM and QD/VM composite nanofibers are prepared by electrospinning. The viscous polymer solutions are loaded in a 10 mL syringe equipped with a 0.80 mm (inner diameter) stainless steel gauge needle. The needle is connected to a high-voltage power supply (Gamma High Voltage Research, Product HV power supply, Model No. ES3UP-5w/DAM), which is capable of providing a DC voltage up to 30 kV. The solution is constantly and continuously supplied using a syringe pump (NE-300, New Era Pump System, Inc.). Various feedrates (*FR*) are studied from 0.5 to 5 μL/min and the optimal feed rate is at 1.5–3.5 μL/min based on the experimental observations. The as-spun fibers, collected from a fixed collector (Fig. 2a), easily adhere each other to form a network or even a thin film structure with a longer time spinning owing to its elastic nature.

To obtain fibers in good quality, a rotating disk collector with a diameter of about 10 cm (Fig. 2b) is used for the electrospinning. The disk is fixed on the shaft of a motor (33A5BEPM, Bodine Electric Company, USA) and the rotation speed can be adjusted from 0 to 2500 rpm/s by a DC motor speed control (WPM-2137E1, Bodine Electric Company, US). The fibers are dried at room temperature in a vacuum oven and stored for further characterization.

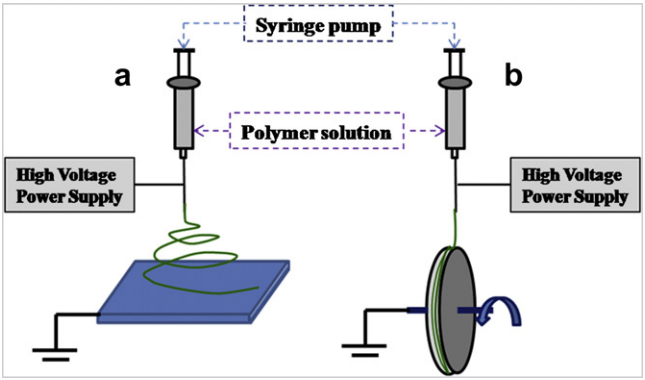

Fig. 2. Schematic electrospinning setup with a (a) fixed and (b) rotating disk electrode.

2.4. Characterization

The rheological behavior of pure VM and QDs suspended VM solutions is investigated with an AR 2000ex Rheometer (TA Instrumental Company) at shear rate ranging from 10 to 1000 l/s at 25 °C. The measurements are performed in a cone-and-plate geometry with a diameter of 40 mm and a truncation of 66 μm.

Fourier transform infrared spectroscopy (FT-IR, Bruker Inc. Vector 22 FT-IR spectrometer, coupled with an ATR accessory) is used to characterize pure VM and its QD/VM composite nanofibers in the range of 500–4000 cm^{-1} at a resolution of 4 cm^{-1}.

UV–Vis spectra of pure VM and its QD/VM nanocomposite toluene solutions are recorded with a 50 bio ultraviolet–visible (UV–Vis) spectrophotometer. The solutions are put in a standard 10 mm path length quartz cuvette for UV–vis test.

Photoluminescence (PL) spectra of VM and its QD/VM nanocomposite solutions are recorded by a Varian CARY Eclipse fluorescence spectrophotometer. All the solutions are diluted to 3% of its original concentration with toluene before measurement. The used excitation wavelength is 350 nm.

The morphology of pure VM and its QD/VM composite nanofibers is evaluated by scanning electron microscopy (SEM, Hitachi S-3400) and further examined in a fluorescent microscope. The fiber samples are prepared by immobilizing the fibers on a glass slide. A cover glass is placed on the slide with a drop of water and sealed. The slides are visualized under different objectives of an Olympus BX51 fluorescence microscope. Images are obtained using Olympus DP72 camera accompanied with Olympus CellSens software.

The thermal stability of pure VM and its QD/VM composite nanofibers with different quantum dots loadings is studied with a thermogravimetric analysis (TGA, TA Instruments TGA Q-500). TGA is conducted from 25 to 700 °C with an air flow rate of 60 mL/min and a heating rate of 10 °C/min. Differential scanning calorimeter measurements (DSC, TA Instruments Q2000) are carried out under a nitrogen flow rate of approximately 100 mL/min and at 10 °C/min heating rate from −25 to 150 °C.

3. Results and discussion

3.1. Rheological behaviors

Fig. 3a & b represents the viscosity (η) as a function of shear rate ($\partial u/\partial y$) of the solutions with four different dispersant concentrations without (Fig. 3a) and with (Fig. 3b) IL. All these samples reveal pseudoplasticity, also known as shear thinning. η is inversely proportional to $\partial u/\partial y$. After comparing Fig. 3a & b, η is relatively higher for the solutions with IL due to a much higher η and surface tension of IL as compared to those of most organic solvents [54]. It is interesting to observe that η of the nanocomposite solutions decreases in a different level depending on the QD loading. In the nanocomposite solution with 1 wt% QD loading, η slightly decreases as compared to that of pure VM solution in both systems with and without IL. With further increasing the QD loading to 3 wt %, the solution experiences a large decrease in η (about 29%, without IL) and even larger decrease (38%, with IL) as compared to that of pure VM solution at the shear rate of 42 l/s. Mackey et al. blended the polystyrene nanoparticles in a linear polystyrene and observed a decreased η, pointing to the introduced free volume by the nanoparticles [55]. And later, they found a similar reduced η in the fullerene/polystyrene and Fe_3O_4/polystyrene nanocomposites with the hypothesis that the nanoparticles merely produce

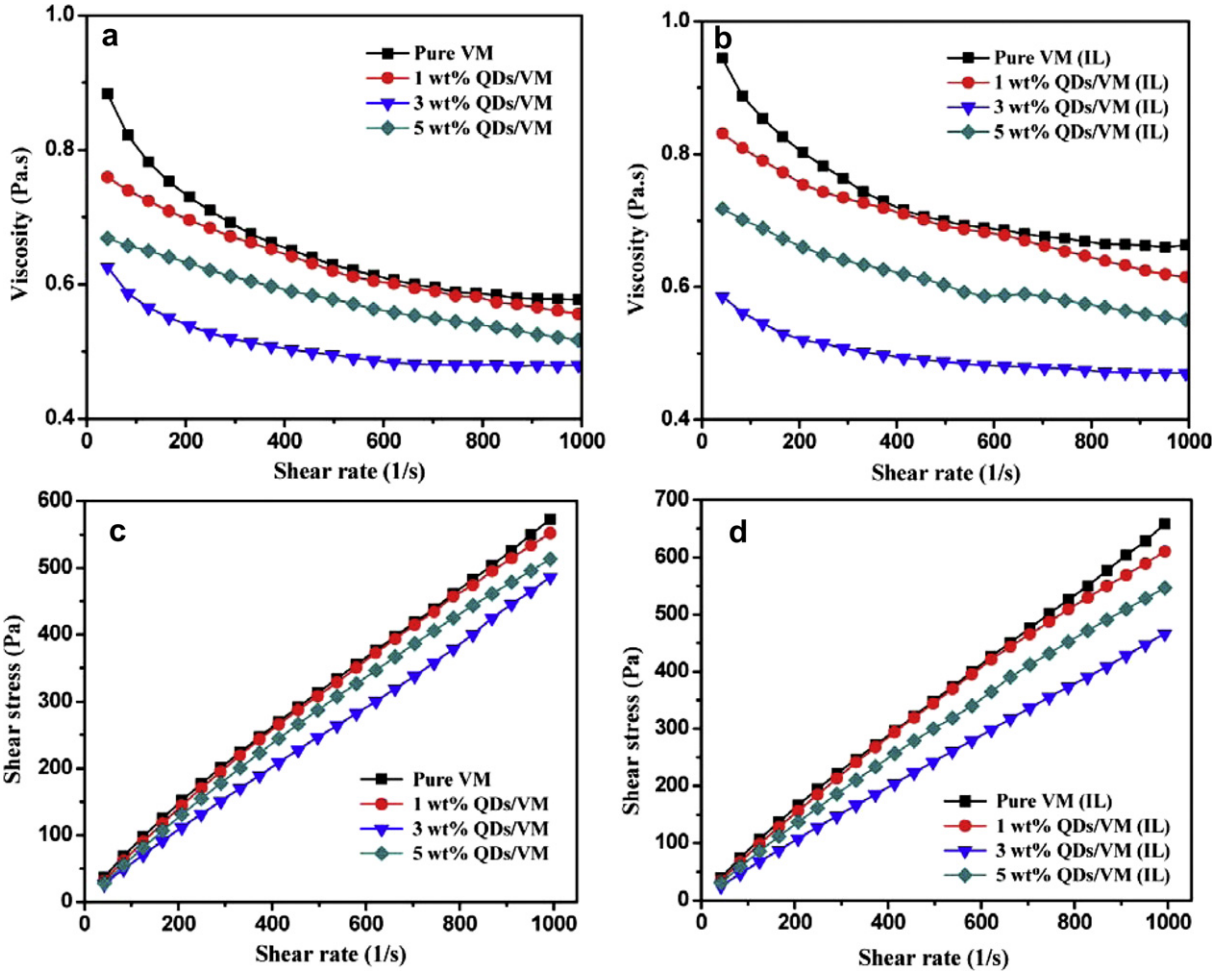

Fig. 3. Viscosity vs shear rate of the solutions (a) without IL and (b) with 1 wt% IL and shear stress vs shear rate of the solutions (c) without IL and (d) with 1 wt% IL.

a dilution effect rather than entanglement owing to their faster diffusion, which provides constraint release and leads to viscosity reduction [56]. Roberts et al. introduced extremely low dimension silica (0.35 nm) in poly(dimethylsiloxane) and found that silica behaves more like solvent rather than particles, which brings the significant reduction in η [57]. In this work, the long alkyl chains of octadecylamine coated on QD surface provide a proper particle spacing with a uniform particle suspension through steric hindrance, which reduces the tendency towards uncontrolled flocculation and leads a decreased η. η increases when the QD loading is 5 wt%, which is due to the enhanced restriction of QDs on the polymer chains derived from a reduced gap distance between QDs or from the slight agglomeration of QDs. The larger aggregates, arising from the conventional solvent evaporation method, clearly offset the nanoscale phenomena with a reduced viscosity observed in a more homogenous fullerene/polystyrene nanocomposites produced by an alternative rapid precipitation method [56]. The unusual η reduction in the spherical QDs suspended elastomer solutions is beneficial for the nanocomposites processing and manufacturing, which is different from other nanofillers, like nanoclays [58], carbon nanofibers (CNFs) [59,60], and carbon nanotubes (CNTs) [61,62], with a significant increased η, a challenge for choosing the processing conditions.

The non-Newtonian fluid behavior of the pure VM and QDs/VM nanocomposites solutions has been modeled using a power law equation from the shear stress (τ)–shear rate ($\partial u/\partial y$) relationship (Fig. 3c and d), eq (2):

$$\tau = K\left(\partial u/\partial y\right)^{n} \tag{2}$$

where K is the flow consistency index, and n is the flow behavior index. For Newtonian fluids, $n = 1$, and $n < 1$ for a pseudoplastic fluid. The values of K, n and standard error (SE) are summarized in Table 1. The K values can be usually related to the fluid viscosity. And the larger deviation of n from 1, the more non-Newtonian behavior the fluids would follow. In Table 1, the K values vary quite consistently with the viscosity curves depending on the QD loading and the addition of IL, as shown in Fig. 3a and b. It is interesting to observe that the solutions filled with 3 wt% QDs with or without IL show the highest n value (>0.93) and the lowest η, which means these solutions show more Newtonian behavior and η is less dependent on the $\partial u/\partial y$. The relatively flat curves, especially at higher $\partial u/\partial y$, for 3 wt% QDs/VM in Fig. 3a and b indicate a tendency of these fluids from non-Newtonian to Newtonian behavior. These fluid behavior changes are essentially important in electrospinning process for choosing the optimal operation conditions, such as feed rate and applying voltage.

3.2. Optical properties

Fig. 4 shows the UV–Vis absorption spectra of CdSe–ZnS QDs aqueous solution, pure VM and QD/VM nanocomposite solutions, respectively. Pure VM shows a flat curve without any absorption

Table 1
The values of *K*, *n* and their standard errors (SE) for VM and QDs/VM toluene solutions.

Composition	*K*	SE	*n*	SE
Pure VM	1.579	0.0450	0.852	0.0043
1 wt% QDs/VM	1.525	0.0391	0.855	0.0039
3 wt% QDs/VM	0.664	0.0399	0.953	0.0091
5 wt% QDs/VM	1.294	0.0423	0.0868	0.0050
Pure VM (IL)	1.417	0.0473	0.888	0.0051
1 wt% QDs/VM (IL)	1.370	0.0787	0.857	0.0072
3 wt% QDs/VM (IL)	0.727	0.0094	0.936	0.0020
5 wt% QDs/VM (IL)	1.245	0.0384	0.883	0.0047

peaks. The QD/VM nanocomposite toluene solution with a QD loading of 5 wt% shows two absorption peaks at 562 and 592 nm, corresponding to the absorption energy of 2.21 and 2.10 eV, respectively ($E = h \times \nu, \nu = c/\lambda$, ν is light wave frequency, s^{-1}; c is light speed, 3×10^8 m s^{-1}; λ is wavelength, m; E is wave energy, eV; h is Planck's constant, $4.135 \times 10 - 15$ eV s), characteristic of a narrow-size distribution of CdSe/ZnS QDs [63]. The measured value shows a blue shift to the band gap of the bulk cubic CdSe (1.77 eV) [64], which is attributed to the small size and the effect of ZnS shell. The nanocomposite solutions show the same peak position as the QDs solution, while the peak intensity decreases with decreasing the QDs loading. The strong band-edge absorption indicates the potential applications of these nanocomposites in the optoelectronic devices [65].

Fig. 5 shows the fluorescence spectra of the diluted pure VM and QD/VM nanocomposite solutions. The inset figure depicts the emission peak of QDs solution at 612 nm with an excitation wavelength of 350 nm. The nanocomposite solutions show the emission peak at the same position with a different intensity, which is well consistent with the characteristic peak of the CdSe–ZnS [66]. Very narrow full width at half-maximum (fwhm) values of 25 nm is observed for both QDs solution and QD/VM solutions, enabling effective distinction between different colors of emission.

3.3. Microstructure of pure VM and composite nanofibers

The slight amount of the ionic liquid introduced in the polymer solution is essentially important for the electrospinning process to obtain the fiber structure. Only spherical dots could be collected on the target without ionic liquid. Fig. 6 shows the structural

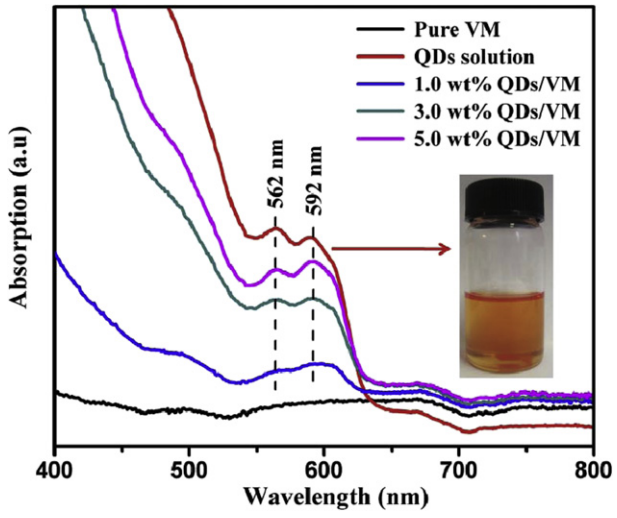

Fig. 4. UV–Vis spectra of pure VM and QDs/VM nanocomposite solutions.

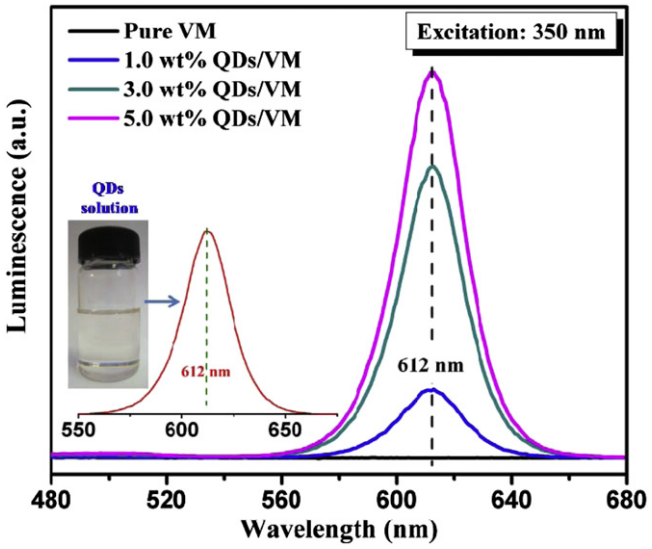

Fig. 5. Fluorescence spectra of pure VM and QDs/VM nanocomposite solutions. The full width at half-maximum (fwhm) is equal to 25 nm. The inset is the fluorescence spectra of the diluted QDs solution.

transformation from the initial fibrous structure (5 min) to the final thin film (30 min) with the extension of spinning time. Fibrous structures combined with some beads are observed at 5 min, and the fibers are partially covered with a continuous polymer phase for 10-min electrospinning. The fibers completely convert to a uniform thin film as the spinning time increases to around 30 min. This observation arises from the flexible non-crystalline elastomer chains, which tend to relax during the electrospinning process and even after deposition on the collector. The accumulated electrospun fibers merge with each other and grow to a continuous thin film with the presence of residual solvent. This is different from the crystalline polymers such as polylactic acid [67], poly acrylic nitrile [2] and polyethylene oxide [68], which are easily electrospun into individual fibers with the advantages of faster solvent evaporation and crystallization through the polymer chain orientation during electrospinning.

To maintain the fibrous structure, pure VM and QD/VM composite nanofibers are produced with a short spinning time, around 5 min. Fig. 7 shows the fibers fabricated from QD/VM nanocomposite solutions with various quantum dots loadings. Owing to a different fluid property such as a decreased viscosity after adding different concentration of QDs (Fig. 3), the electrospinning process has been optimized through adjusting the operational parameters, such as applied electrical voltage, tip-to-collector distance and *FR*. Generally, the surface tension force together with the viscoelastic force of the solution should be balanced with the electrostatic force to obtain stable jets, which are required for the fiber formation. Once the applied voltage exceeds the critical voltage, the stable jets of liquid will be ejected from the cone tip. However, the efforts still seem to be unfavorable for fabricating high quality individually separated fibers. Instead, the fibers connect with each other and form a network structure due to the elastic nature of the elastomer. Both micron- and nano-fibers are observed, which is attributed to the fiber splaying during the spinning process [1,69]. Meanwhile, it is impossible to exclude the possibility that the microscale fibers are merged from nanoscale fibers.

With the aim to obtain better quality aligned individually separated fibers, the electrospinning setup is modified by replacing the fixed collector with a rotating disk collector, which is driven by a speed controllable motor. Single aligned fibers (diameter <1 μm) rather than network structure are observed, Fig. 8. The relatively

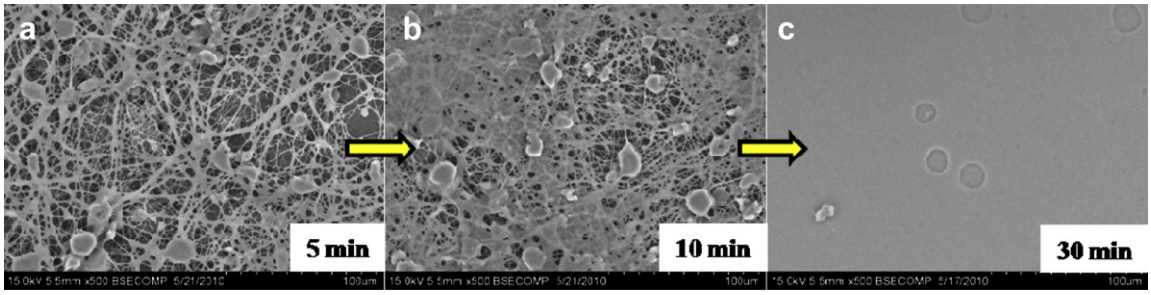

Fig. 6. The morphology evolution from VM fiber structure to thin film with an elongation of the spinning time (*Feedrate*: 3.5 μl/min, *Voltage*: 15 kV, *Distance*: 25 cm).

narrow edge (~1 cm) of the disc collector affects the electrostatic force field and exerts a pulling force on the polymer jets. In addition, the rotation of the wheel has an effect on the fibers once they touch the wheel and wound around its edge. The tangential force, acting on the fibers, further stretches the collecting fibers and consequently reduces the diameter to nanometer, Fig. 8. The fibers are highly oriented (along the marking arrow), which is revealed by the uniformly colored composite nanofibers in fluorescence microscopy images, Fig. 9. The fluorescence images, taken in both bright field and dark field, are compared in Fig. 9. The composite nanofibers with 1 wt% quantum dots loading do not show any emission signal in the dark field due to a lowered intensity of the fluorescence in the polymer matrix, which cannot be detected by the used equipment. However, the aligned fibers with a strong and uniform red emission signal are observed when the QD loading increases to 3 and 5 wt%, indicating a good distribution of the QDs within the matrix.

3.4. FT-IR analysis

FT-IR analysis is used to disclose whether chemical bonding or physical entanglement occurs between the QDs and VM in the fibers after the blending and electrospinning processes. Fig. 10a shows the FT-IR spectra of pure VM fibers. The major absorption bands at 2750–3000 cm^{-1} and 1250–1500 cm^{-1} correspond to the vibration of C–H and $-CH_3$ of polypropylene (PP), respectively, which are in good agreement with the PP/clay nanocomposites and PP/polyvinyl alcohol blends [70–72]. For references, the VM thin film without IL (Fig. 10e) and pure IL (Fig. 10f) are also tested. The broad peak at 1064 cm^{-1} in the fibers (Fig. 10a–d) is from IL and the two small peaks on its shoulder indicate the characteristic absorption of polyethylene [73]. The characteristic peaks of IL can be identified from the electrospun fibers (marked with arrows) and the specific peak value of each peak can be observed on the IL curve (Fig. 10f). In addition, the characteristic peaks of VM are still

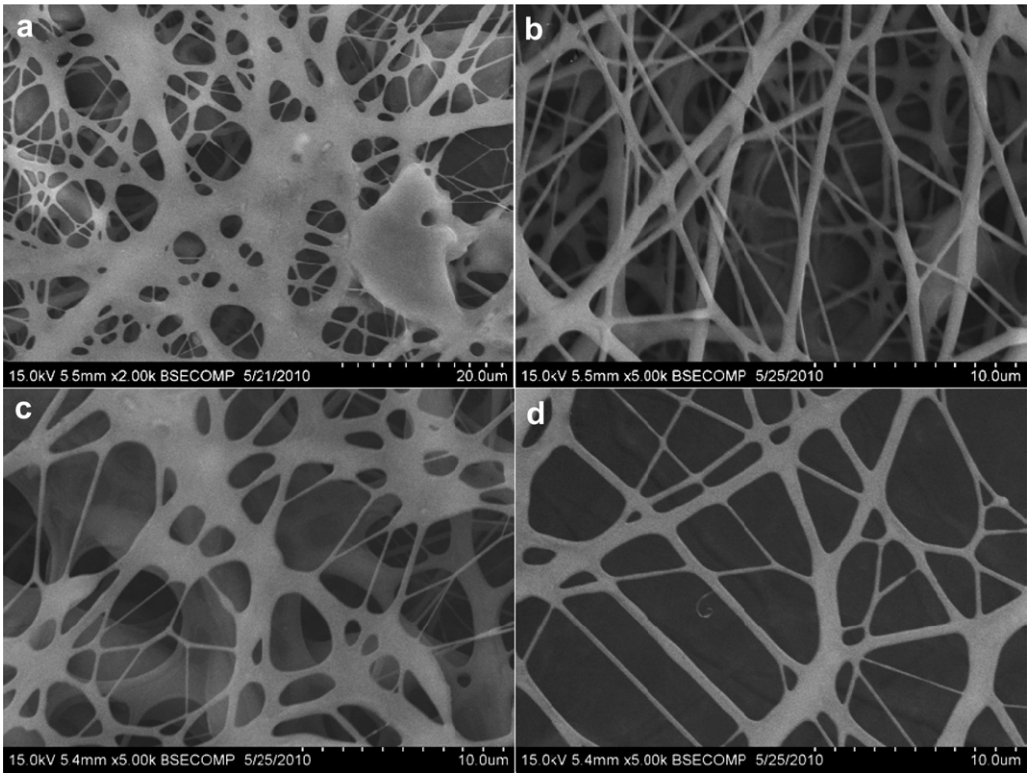

Fig. 7. SEM microstructures of the fibers using fixed collector (a) pure VM, and composite nanofibers with a quantum dots loading of (b) 1, (c) 3, and (d) 5 wt%. (Samples are produced from different operational conditions: (a) 3.5 μl/min, 15 kV, 25 cm; (b) 2.5 μl/min, 18 kV, 25 cm; (c) 2.5 μl/min, 15 kV, 25 cm; and (d) 3.5 μl/min, 15 kV, 30 cm). Collecting time: 5 min.

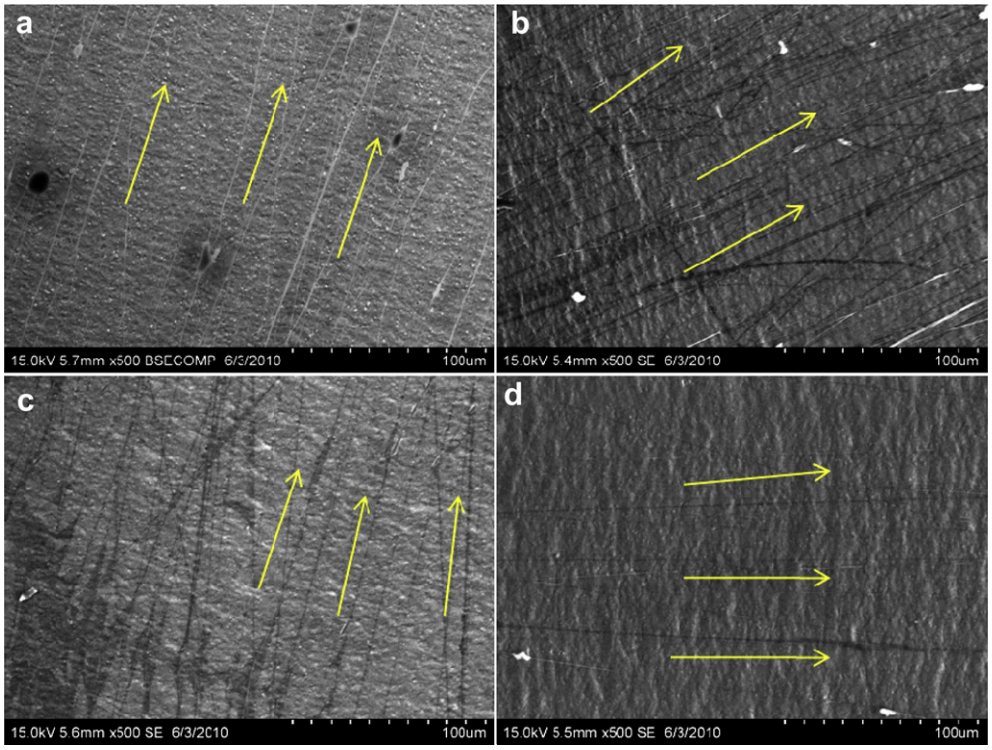

Fig. 8. SEM microstructures of the aligned fibers using a rotating disk electrode: (a) pure VM, and composite nanofibers with a quantum dots loading of (b) 1, (c) 3, and (d) 5 wt%. (The rough background is aluminum foil, yellow arrows indicate the aligned direction of the fibers, spinning conditions are: 2.5 μl/min, 15 kV, 20 cm, rotation speed: 1500 rpm).

maintained after the electronspinning process. Compared with the absorption curve of pure VM fibers, no additional bands are observed in composite nanofibers, Fig. 10b–d, which is due to the dominating phase of the VM in the nanocomposites.

3.5. Thermalgravimetric analysis

Fig. 11 shows the thermal gravimetric curves of pure VM and its QD/VM composite nanofibers up to 700 °C. The 5% and 10% weight loss temperatures as well as the onset decomposition temperature are obtained and summarized in Table 2. All these obtained values indicate an enhanced thermal stability of the composite nanofibers with increasing QD loading. As compared to that of pure VM, the 5 wt% QDs/VM composite nanofibers exhibit higher thermal stability with an enhanced decomposition temperature about 14.8, 17.1 and 26.5 °C for $T_{5\%}$, $T_{10\%}$ and T_{onset}, respectively. The enhanced decomposition temperature is due to the restriction of the QDs on the long range chain mobility of the polymer phase within the composite nanofibers. Generally, the nanoparticle restriction requires a uniform distribution of the nanofillers within the polymer matrix, which is evidenced by the fluorescence images with uniformly colored composite nanofibers, Fig. 9. Similar results are also reported in other polymer nanocomposite systems with the incorporation of various nanomaterials in different polymer matrix,

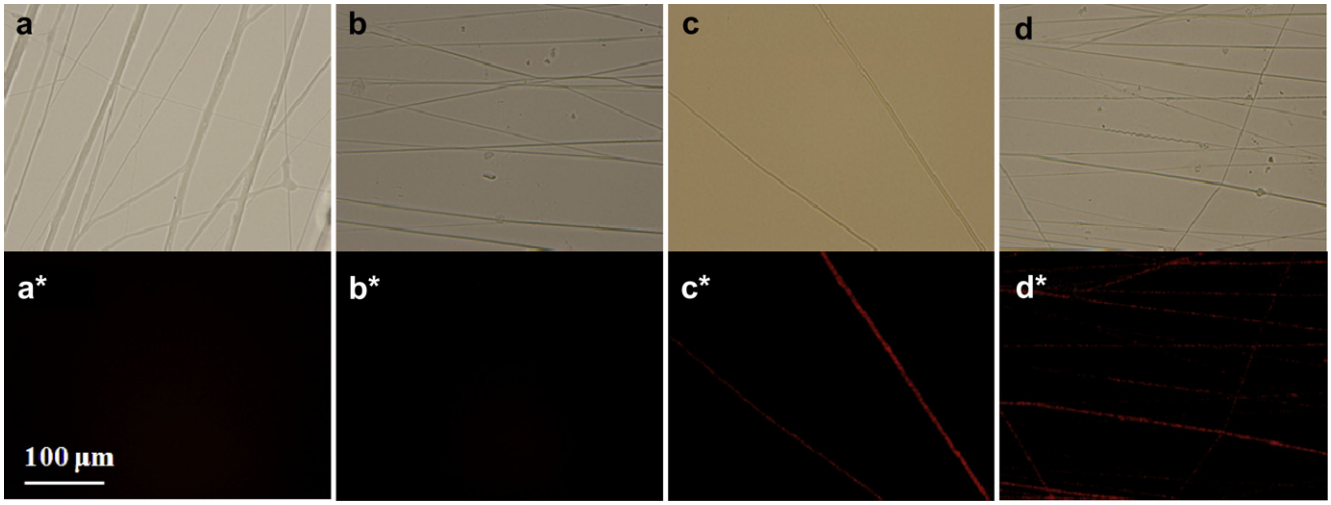

Fig. 9. Bright field fluorescence microscopy images of (a) pure VM, and composite nanofibers with a quantum dots loading of (b) 1, (c) 3 and (d) 5 wt%. a*–d* correspond to a–d in dark field. (the scale bar is suitable for each image).

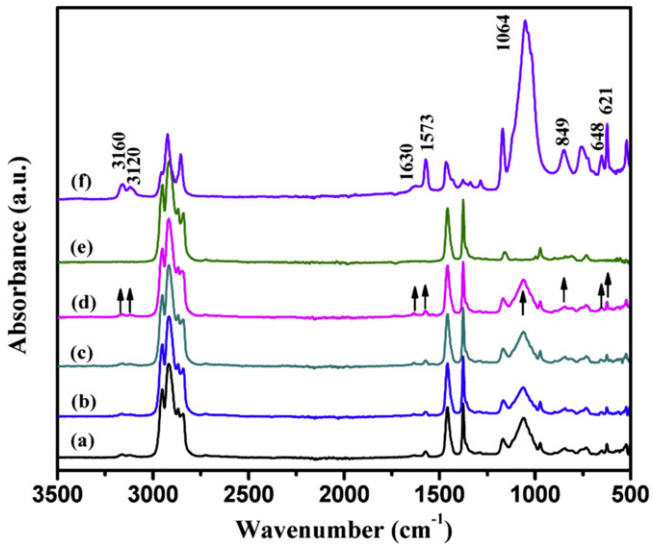

Fig. 10. FT-IR spectra of the IL assisted electrospun fibers of (a) pure VM, and QDs/VM nanocomposites with a quantum dots loading of (b) 1, (c) 3 and (d) 5 wt%; and (e) VM thin film without IL and (f) pure IL, respectively.

such as carbon nanofibers/epoxy [60], core@shell structured Fe@FeO nanoparticles reinforced polyimide composite nanofibers [1] and iron oxide/polypyrrole nanocomposites [74].

3.6. DSC analysis

The DSC curves of pure VM and QD/VM composite nanofibers, Fig. 12, exhibit three different peaks at around −4 °C, 50 °C and 110 °C, respectively. The glass transition temperature (T_g) is almost constant with the addition of the QDs, while a small peak (marked with arrows) appears on the right shoulder of the glass transition peak for the composite nanofibers filled with 3 and 5 wt% QDs, respectively, which may come from the melting of the surfactant octadecylamine (melting temperature, T_m = 52.9 °C) used for the stabilization of QDs. The T_m is observed to increase by 2 and 4.1 °C with the addition of 1 and 3 wt% QDs as compared to that (109.1 °C) of pure VM, suggesting a restriction of the QDs on the polymer chains. With further increasing the particle loading to 5 wt%, the T_m decreases but still comparable to that of pure VM. This observation is consistent with the viscosity change with the variation of the particle loadings, Fig. 12, indicating a structural change of the polymer nanocomposites. It is interesting to notice that only the latter two peaks are observed for the thin films, Fig. 13, which correspond to the glass transition and melting behavior of the elastomer, respectively. To be specific, VM thin films are prepared by using a solvent evaporation method without ionic liquid to compare the thermal behaviors between the fibers and the thin

Table 2
TGA results of pure VM and QDs/VM nanocomposites.

Samples	$T_{5\%}$ (°C)	$T_{10\%}$ (°C)	T_{onset} (°C)
Pure VM	242.7	264.2	226.6
1 wt% QDs/VM	249.7	271.0	235.3
3 wt% QDs/VM	255.3	275.8	238.4
5 wt% QDs/VM	257.5	281.3	253.1

$T_{5\%}$ and $T_{10\%}$ indicate the specific temperature at 5% and 10% weight loss, respectively. T_{onset} means the onset degradation temperature.

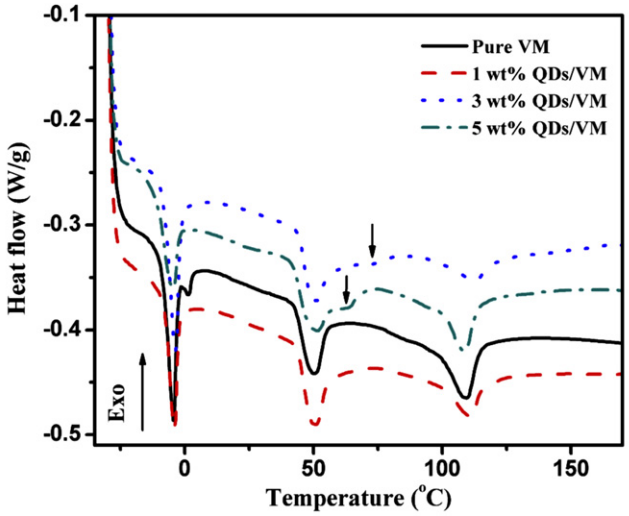

Fig. 12. DSC thermograms of pure VM and QDs/VM composite nanofibers with different quantum dots loadings.

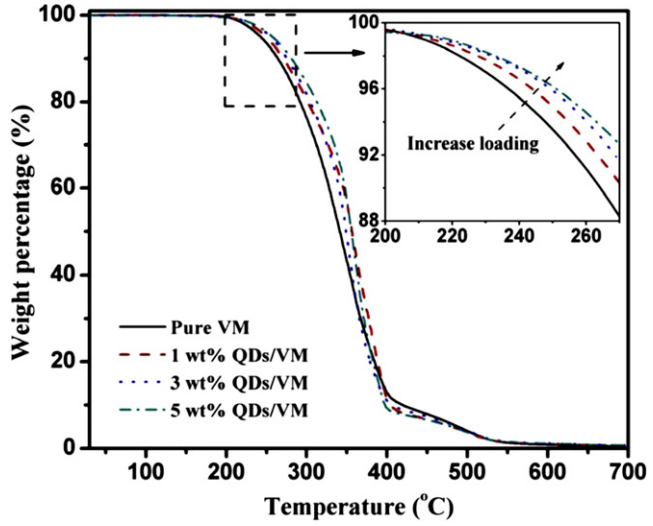

Fig. 11. TGA curves of pure VM and QDs/VM composite nanofibers with different quantum dots loadings (the inset figure is magnified from 200 to 270 °C).

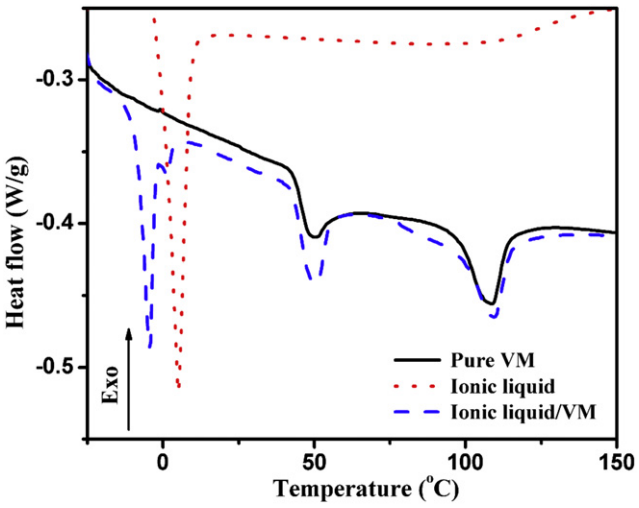

Fig. 13. DSC thermograms of pure VM thin film without IL, pure IL and electrospun VM fibers containing IL.

films. And similar glass transition and melting behavior are observed, Fig. 13. However, the sharp peak at around −4 °C of the IL/VM fibers arises from the melting temperature of ionic liquid, which is 8 °C lower than that of the pure ionic liquid after mixing with the polymer. The lowered T_m is due to the reduced static force resulting from the dissociation of positive and negative ions. These observations suggest that a strong interaction exists between the polymer chains and ionic liquid after the electrospinning process.

4. Conclusion

With the aid of ionic liquid to increase the ionic strength of the polymer solution, aligned luminescent elastomer composite nanofibers filled with quantum dots are produced using the simple electrospinning method. Both fixed and rotating disk electrodes are used to collect the fibers. The fibers easily merge together and finally transform to an elastomer thin film while using the fixed collector. However, separately aligned QDs/VM individual fibers are successfully collected using a rotating disk electrode. The fluorescence images from the aligned fibers reveal that the QDs are uniformly dispersed within the polymer fiber matrix and the strong emission signal with a fiber structure provides them the great potential for bio-applications [9,38,67]. The UV–Vis absorption and photoluminescent properties of the QDs/VM nanocomposite solutions indicate that the optical performance of the QDs is not affected after dispersing in the polymer. DSC results on the fibers reveal the interaction between ionic liquid and the polymer chains, which facilitates the electrospinning process. And TGA results of the composite nanofibers show an enhanced thermal stability as compared to that of the pure polymer fibers. Higher thermal decomposition temperature is observed in the composite nanofibers with a higher particle loading.

Acknowledgements

This project is partially supported by the National Science Foundation-Nanoscale Interdisciplinary Research Team and Materials Processing and Manufacturing (CMMI-1030755). The elastomer supplied from ExxonMobil Chemical Company is greatly appreciated.

References

[1] Zhu J, Wei S, Chen X, Karki AB, Rutman D, Young DP, et al. J Phys Chem C 2010;114:8844–50.
[2] Zhang D, Karki AB, Rutman D, Young DP, Wang A, Cocke D, et al. Polymer 2009;50:4189–98.
[3] Reneker DH, Chun I. Nanotechnology 1996;7:216–23.
[4] Kim GM, Wutzler A, Radusch HJ, Michler GH, Simon P, Sperling RA, et al. Chem Mater 2005;17:4949–57.
[5] Teo WE, Ramakrishna S. Nanotechnology 2006;17:R89–106.
[6] Wang D, Li K, Teo WK. J Memb Sci 1996;115:85–108.
[7] Ma Z, Kotaki M, Ramakrishna S. J Memb Sci 2006;272:179–87.
[8] Buchko CJ, Chen LC, Shen Y, Martin DC. Polymer 1999;40:7397–407.
[9] Zong X, Bien H, Chung CY, Yin L, Fang D, Hsiao BS, et al. Biomaterials 2005;26:5330–8.
[10] Ramakrishna S, Fujihara K, Teo WE, Lim TC, Ma Z. An introduction to electrospinning and nanofibers. Singapore: World Scientific; 2005.
[11] Pelrine R, Kornbluh R, Pei Q, Joseph J. Science 2000;287:836–9.
[12] Kim S, Aksak B, Sitti M. Appl Phys Lett 2007;91:221913.
[13] Puskas JE, Chen Y. Biomacromolecules 2004;5:1141–54.
[14] Yun KM, Hogan Jr CJ, Matsubayashi Y, Kawabe M, Iskandar F, Okuyama K. Chem Eng Sci 2007;62:4751–9.
[15] Qin YJ. Appl Polym Sci 2006;100:2516–20.
[16] Sill TJ, von Recum HA. Biomaterials 2008;29:1989–2006.
[17] Zeng J, Xu X, Chen X, Liang Q, Bian X, Yang L, et al. J Controlled Release 2003;92:227–31.
[18] Yoshimoto H, Shin YM, Terai H, Vacanti JP. Biomaterials 2003;24:2077–82.
[19] Li WJ, Laurencin CT, Caterson EJ, Tuan RS, Ko FK. J Biomed Mater Res 2002;60:613–21.
[20] Ding W, Wei S, Zhu J, Chen X, Rutman D, Guo Z. Macromol Mater Eng 2010;295:958–65.
[21] Chen X, Wei S, Gunesoglu C, Zhu J, Southworth CS, Sun L, et al. Macromol Chem Phys 2010;211:1775–83.
[22] Huang ZM, Zhang YZ, Kotaki M, Ramakrishna S. Compos Sci Technol 2003;63:2223–53.
[23] Teo WE, Ramakrishna S. Nanotechnology 2006;17:R89–106.
[24] Choi SS, Hong JP, Chung SM, Nah C. J Appl Polym Sci 2006;101:2333–7.
[25] Fang J, Lin T, Tian W, Sharma A, Wang XJ. J Appl Polym Sci 2007;105:2321–6.
[26] Brown SB. In: Utracki LA, editor. Polymer blends handbook. London: Kluwer Academic; 2002.
[27] Hu K, Brust M, Bard AJ. Chem Mater 1998;10:1160–5.
[28] Robel I, Subramanian V, Kuno M, Kamat PV. J Am Chem Soc 2006;128:2385–93.
[29] Gaponik NP, Talapin DV, Rogach AL. Phys Chem Chem Phys 1999;1:1787–9.
[30] Mattoussi H, Mauro JM, Goldman ER, Anderson GP, Sundar VC, Mikulec FV, et al. J Am Chem Soc 2000;122:12142–50.
[31] Michalet X, Pinaud FF, Bentolila LA, Tsay JM, Doose S, Li JJ, et al. Science 2005;307:538–44.
[32] Voura EB, Jaiswal JK, Mattoussi H, Simon SM. Nat Med 2004;10:993–8.
[33] Chan WCW, Nie S. Science 1998;281:2016–8.
[34] Schaller RD, Klimov VI. Phys Rev Lett 2004;92:186601.
[35] Murphy JE, Beard MC, Norman AG, Ahrenkiel SP, Johnson JC, Yu P, et al. J Am Chem Soc 2006;128:3241–7.
[36] Kikkeri R, Lepenies B, Adibekian A, Laurino P, Seeberger PH. J Am Chem Soc 2009;131:2110–2.
[37] Kim S, Lim YT, Soltesz EG, De Grand AM, Lee J, Nakayama A, et al. Nat Biotechnol 2004;22:93–7.
[38] Mo XM, Xu CY, Kotaki M, Ramakrishna S. Biomaterials 2004;25:1883–90.
[39] Keun Kwon I, Kidoaki S, Matsuda T. Biomaterials 2005;26:3929–39.
[40] Yang F, Murugan R, Wang S, Ramakrishna S. Biomaterials 2005;26:2603–10.
[41] Zhu J, Wei S, Zhang L, Mao Y, Ryu J, Karki AB, et al. J Mater Chem 2011;21:342–8.
[42] Zhu J, Wei S, Zhang L, Mao Y, Ryu J, Haldolaarachige N, et al. J Mater Chem 2011;21:3952–9.
[43] Zhu J, Wei S, Ryu J, Sun L, Luo Z, Guo Z. ACS Appl Mater Interfaces 2010;2:2100–7.
[44] Liu H, Edel JB, Bellan LM, Craighead HG. Small 2006;2:495–9.
[45] Choudhury KR, Sahoo Y, Ohulchanskyy TY, Prasad PN. Appl Phys Lett 2005;87:073110.
[46] Shenoy DK, Laurence Thomsen Iii D, Srinivasan A, Keller P, Ratna BR. Sens Actuators, A 2002;96:184–8.
[47] Thomsen DL, Keller P, Naciri J, Pink R, Jeon H, Shenoy D, et al. Macromolecules 2001;34:5868–75.
[48] Ranke J, Stolte S, Sörmann R, Arning J, Jastorff B. Chem Rev 2007;107:2183–206.
[49] Zhu S, Wu Y, Chen Q, Yu Z, Wang C, Jin S, et al. Green Chem 2006;8:325–7.
[50] Hu H, Yang H, Huang P, Cui D, Peng Y, Zhang J, et al. Chem Commun 2010;46:3866–8.
[51] Lin J, Ding B, Yu J, Hsieh Y. ACS Appl Mater Interfaces 2010;2:521–8.
[52] Lu X, Zhou J, Zhao Y, Qiu Y, Li J. Chem Mater 2008;20:3420–4.
[53] Viswanathan G, Murugesan S, Pushparaj V, Nalamasu O, Ajayan PM, Linhardt RJ. Biomacromolecules 2006;7:415–8.
[54] Xu S, Zhang J, He A, Li J, Zhang H, Han CC. Polymer 2008;49:2911–7.
[55] Mackay ME, Dao TT, Tuteja A, Ho DL, Van Horn B, Kim HC, et al. Nat Mater 2003;2:762–6.
[56] Tuteja A, Duxbury PM, Mackay ME. Macromolecules 2007;40:9427–34.
[57] Roberts C, Cosgrove T, Schmidt RG, Gordon GV. Macromolecules 2001;34:538–43.
[58] Lepoittevin B, Devalckenaere M, Pantoustier N, Alexandre M, Kubies D, Calberg C, et al. Polymer 2002;43:4017–23.
[59] Zhu J, Wei S, Yadav A, Guo Z. Polymer 2010;51:2643–51.
[60] Zhu J, Wei S, Ryu J, Budhathoki M, Liang G, Guo Z. J Mater Chem 2010;20:4937–48.
[61] Hu G, Zhao C, Zhang S, Yang M, Wang Z. Polymer 2006;47:480–8.
[62] Mitchell CA, Bahr JL, Arepalli S, Tour JM, Krishnamoorti R. Macromolecules 2002;35:8825–30.
[63] Baranov AV, Rakovich YP, Donegan JF, Perova TS, Moore RA, Talapin DV, et al. Phys Rev B 2003;68:165306.
[64] Pan A, Yang H, Liu R, Yu R, Zou B, Wang Z. J Am Chem Soc 2005;127:15692–3.
[65] Sun Q, Wang YA, Li LS, Wang D, Zhu T, Xu J, et al. Nat Photon 2007;1:717–22.
[66] Dorokhin D, Tomczak N, Han M, Reinhoudt DN, Velders AH, Vancso GJ. ACS Nano 2009;3:661–7.
[67] Badami AS, Kreke MR, Thompson MS, Riffle JS, Goldstein AS. Biomaterials 2006;27:596–606.
[68] Deitzel JM, Kleinmeyer JD, Hirvonen JK, Beck Tan NC. Polymer 2001;42:8163–70.
[69] Deitzel JM, Kleinmeyer J, Harris D, Beck Tan NC. Polymer 2001;42:261–72.
[70] Qin H, Zhang S, Zhao C, Hu G, Yang M. Polymer 2005;46:8386–95.
[71] Qin H, Zhang S, Liu H, Xie S, Yang M, Shen D. Polymer 2005;46:3149–56.
[72] Jang J, Lee DK. Polymer 2004;45:1599–607.
[73] Wang KH, Choi MH, Koo CM, Choi YS, Chung IJ. Polymer 2001;42:9819–26.
[74] Guo Z, Shin K, Karki AB, Young DP, Kaner RB, Hahn HT. J Nanopart Res 2009;11:1441–52.